

Second harmonic generation of semiorganic dichlorobis(L-proline)zinc(II) single crystals for laser applications

D. KALAISELVI*, R. JAYAVEL^a

Department of Physics, Queen Mary's College, Chennai- 600 004, India

^aCrystal Growth Centre, Anna University, Chennai - 600 025, India

A potentially useful semiorganic nonlinear optical material, dichlorobis (L-proline)zinc(II), has been synthesized and bulk crystals have been grown by slow cooling technique. Good quality single crystal of size $18 \times 6 \times 3 \text{ mm}^3$ has been grown over a period of 15 days. The grown crystal was characterized by single crystal X-ray diffraction, Fourier transform infrared, Ultraviolet-visible spectroscopy and thermal analysis. The grown crystals were thermally stable upto 247.4°C and exhibit second harmonic generation efficiency of about 1.5 times that of potassium dihydrogen phosphate. The step growth pattern along (010) plane of the crystal was observed using scanning electron microscopy. The elemental composition was analyzed and the presence of zinc and chlorine in the title compound was confirmed by energy dispersive X-ray analysis.

(Received January 4, 2011; accepted January 26, 2011)

Keywords: Growth from solutions, Crystal growth, Nonlinear optical materials

1. Introduction

Semiorganic nonlinear optical (NLO) materials are reputed candidates for device fabrication, owing to their large nonlinear coefficient, high laser damage threshold and exceptional mechanical and thermal stabilities. Semiorganic materials are metal-organic coordination compounds, in which the organic ligand plays a dominant role in the NLO effect. As for the metallic part, the focus is on group II B metals (Zn, Cd and Hg) as these compounds usually have a high transparency in the UV region, because of their closed shell [1-2]. In the organometallic complexes, the metal centre is engaged in Π -bonding with the organic ligating groups and can be involved in strongly allowed metal to ligand charge transfer (MLCT), which leads to excellent second harmonic generation (SHG) devices. Efficient SHG has been mostly limited to noncentrosymmetric crystals. However, SHG in some centrosymmetric crystals would be allowed because of the breaking of inversion symmetry at the surface of the particle. Hence, second harmonic light may be reflected from the interface of the two centrosymmetric media [3]. Recently, several complexes of proline were reported such as L-proline cadmium chloride monohydrate and L-proline lithium chloride monohydrate [4-5]. Proline is an abundant amino acid in collagen and is exceptional among the amino acids because it is the only one in which the amine group is part of a pyrrolidine ring, thus making it rigid and directional in biological systems [6]. In this present communication, we report the synthesis and solubility measurement of dichlorobis(L-proline)zinc(II) [DBLPZ]. Bulk crystal of

size $18 \times 6 \times 3 \text{ mm}^3$ has been grown with optimized growth condition. The grown crystals have been characterized by single crystal X-ray diffraction analysis, FTIR, optical, thermal, SEM, EDAX and NLO studies.

2. Experimental procedure

2.1 Synthesis and purification of DBLPZ

DBLPZ was synthesized by the reaction between L-proline and zinc chloride taken in the stoichiometric ratio of 2:1. The calculated amount of zinc chloride was first dissolved in millipore water. L-proline was then slowly added to the solution and stirred well using a temperature controlled magnetic stirrer to yield a homogeneous mixture of solution. Then, the solution was allowed to evaporate at room temperature, which yielded the crystalline salt of DBLPZ. The purity of the synthesized salt was improved by successive recrystallization process.

2.2 Solubility studies

Solubility is one the most important parameters for the growth of good quality crystals in low temperature solution growth method. The solubility of DBLPZ was determined for four different temperatures 30, 35, 40 and 45°C by dissolving the solute in millipore water in an airtight container maintained at a constant temperature with stirring.

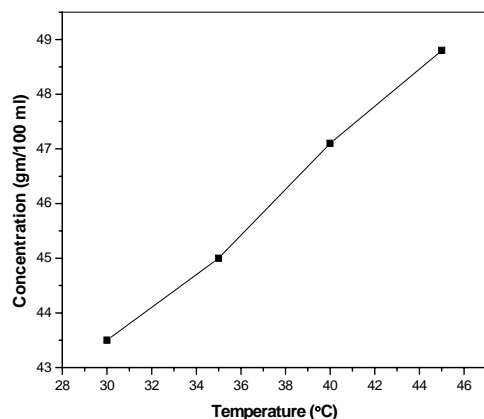


Fig. 1. Solubility curve of DBLPZ in aqueous solution.

After saturation was attained, the equilibrium concentration of the solute was analyzed gravimetrically. The same procedure was repeated to estimate the solubility for different temperatures. Fig. 1 shows the solubility curve of DBLPZ in aqueous solution.

2.3 Crystal growth of DBLPZ

The starting material of DBLPZ was dissolved in millipore water in accordance with the solubility data. The saturated solution of DBLPZ was prepared at 40°C and the solution was filtered to remove any impurities. Good optical quality seed crystals obtained by slow evaporation method were used for the bulk growth. The growth was carried out in a constant temperature bath of controlling accuracy $\pm 0.01^\circ\text{C}$. A cooling rate of $0.2^\circ\text{C}/\text{day}$ was employed during the initial and final stages of the growth period. Optical quality crystal of dimension $18 \times 6 \times 3 \text{ mm}^3$ has been grown over a typical growth period of 15 days. As grown single crystal of DBLPZ is shown in Fig. 2.

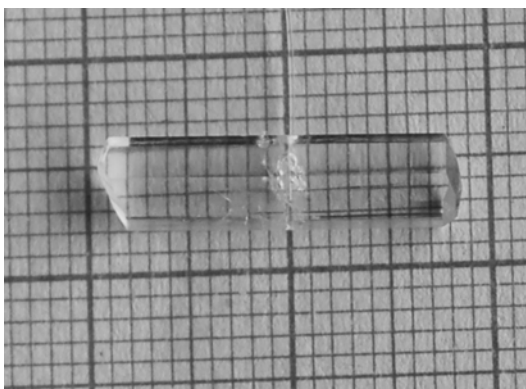


Fig. 2. As grown DBLPZ single crystal with dimension of $18 \times 6 \times 3 \text{ mm}^3$ from aqueous solution pH of 4.0.

3. Results and discussion

3.1 Single crystal X-ray diffraction analysis

The grown crystals were subjected to single crystal X-ray diffraction analysis using ENRAF NONIUS CAD-4 X-ray diffractometer with $\text{MoK}\alpha$ ($\lambda = 0.71069 \text{ \AA}$) radiation. This study reveals that the grown crystal belongs to orthorhombic system with the space group $\text{P}2_12_12_1$ and $Z = 4$. The lattice parameter values are $a = 6.559 (8) \text{ \AA}$, $b = 13.422 (10) \text{ \AA}$, $c = 16.238 (9) \text{ \AA}$, $\alpha = \beta = \gamma = 90^\circ$ and volume = $1429.5 (5) \text{ \AA}^3$, which is in good agreement with the reported value [7]. Fig. 3 shows the ORTEP diagram of DBLPZ crystal. The zinc atom is coordinated in a tetrahedral geometry to two chlorine atoms and the two carboxyl oxygen atoms of two L-proline ligands. Each L-proline is coordinated as a monodentate ligand.

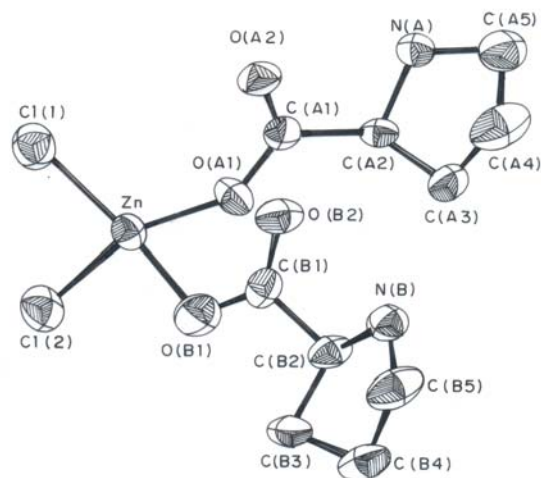


Fig. 3. ORTEP diagram of DBLPZ crystal.

3.2 Morphology studies

Fig. 4 shows the morphology of the as grown DBLPZ single crystal. It is observed that the growth rate along the a-axis is much higher than that of b and c-axes, which resulted elongation along $[100]$ direction. The a-axis lies along the length of the crystal. The (010) plane is the most prominent plane and (001) , $(10 \bar{2})$, $(10 \bar{2})$ are the other well-developed planes.

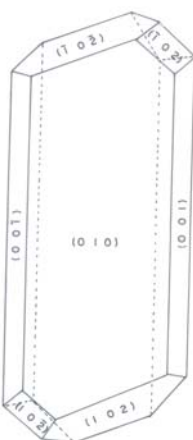


Fig. 4. Morphology of DBLPZ single crystal.

3.3 Optical absorption studies

The optical absorption spectrum of DBLPZ was recorded using a Varian Cary 5E Spectrophotometer in the range 200 – 800 nm as shown in the Fig. 5. The absorbance is found to be very low in the entire visible region, which is one of the most desired properties for the materials possessing SHG. From the spectrum, the UV cut-off wavelength is found to be 235 nm.

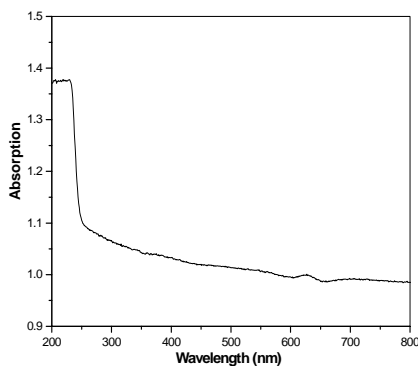


Fig. 5. Optical absorption spectrum of DBLPZ crystal.

3.4 FTIR analysis

The FTIR spectrum of DBLPZ crystal was recorded in the range 400 – 4000 cm^{-1} using Bruker IFS 66V by KBr pellet technique. Fig. 6 shows the FTIR spectrum of DBLPZ crystal. The peaks at 3153 and 3028 cm^{-1} are due to N-H vibrations. The asymmetric and symmetric vibrations of COO^- occur at 1668 and 1412 cm^{-1} respectively. The $[\text{NH}_2]^+$ and COO^- scissoring gives its peaks at 1559 and 677 cm^{-1} . The peak at 1374 cm^{-1} is assigned to C-H bending. The CH_2 twisting mode occurs at 1331 and 1169 cm^{-1} . The wagging and rocking of CH_2 are observed at 1265, 1037 and 846 cm^{-1} . The C-C and C-N stretching modes give a peak at 941 cm^{-1} . The peaks

at 779 and 596 cm^{-1} are assigned to skeletal deformation of pyrrolidine ring and on comparison of the spectra with L-proline illustrates the shift in peak position as well as the change in the intensity of the peak below 1400 cm^{-1} . It is evident that the spectrum is different from that of pure L-proline, and hence L-proline interacts with ZnCl_2 , which also has support from the XRD analysis.

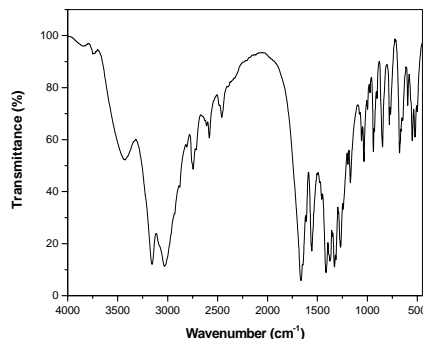


Fig. 6. FTIR spectrum of DBLPZ.

3.5 Thermal analysis

Differential thermal analysis (DTA), Thermogravimetric analysis (TGA) and Differential scanning calorimetry (DSC) of DBLPZ crystals were carried out simultaneously using NETZSCH – Geratebau GmbH thermal analyser. A powder sample was used for these analyses in the temperature range of 27 to 1200 $^{\circ}\text{C}$ with a heating rate of 20 K/min in an inert nitrogen atmosphere. The alumina crucible was used as the reference. The characteristic curves of TGA, DTA and DSC are shown in Fig. 7a and Fig. 7b. From the TGA curve, it is observed that the compound starts to lose single molecule of amino group at about 247 $^{\circ}\text{C}$ and continues upto 453 $^{\circ}\text{C}$. A second dissociation occurred between 453 – 820 $^{\circ}\text{C}$ due to removal of another molecule of amino group and the third dissociation started at above 820 $^{\circ}\text{C}$ with evolution of carbon dioxide. The percentage of residue obtained at 1199 $^{\circ}\text{C}$ is equal to 4.26. Since there is no weight loss below 150 $^{\circ}\text{C}$, the lattice is free of any adsorbed water in the crystal.

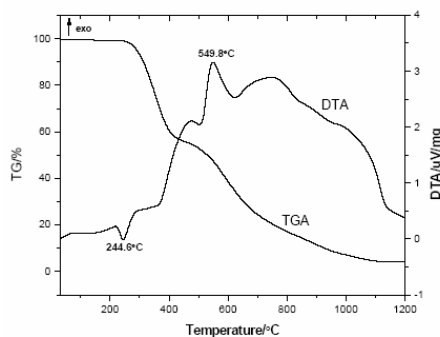


Fig. 7a. TGA and DTA curves of DBLPZ.

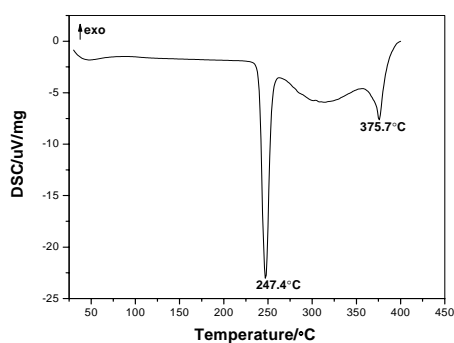


Fig. 7b. DSC curve of DBLPZ.

In the DTA curve, the endothermic peak at 244.6 °C corresponds to melting point of the substance and then it undergoes an exothermic peak at 549.8 °C, which is associated with weight loss as observed from the TGA curve. From the DSC curve, the crystal of DBLPZ was stable upto its melting point 247.4 °C.

3.6 Surface features and composition analysis

The surface features of the crystal was observed by a scanning electron microscopy (SEM) using a Hitachi scanning electron microscope analyser operated at 3 kV for different magnifications on the (010) plane, after coating the sample with gold layer using Hitachi Vacuum Evaporator. The obtained micrograph of the DBLPZ crystal is shown in Fig. 8. From the micrograph, it is observed that the growth surface shows step growth along (010) plane of the DBLPZ crystal.

An elemental analysis was carried out for DBLPZ by the energy dispersive X-ray analysis (EDAX) in order to confirm the composition of zinc and chlorine radicals in the crystal. Fig. 9 illustrates the EDAX spectrum of DBLPZ crystal recorded with gold coating, which suggest the percentage of zinc and chlorine present in the crystal lattices of the DBLPZ single crystal.

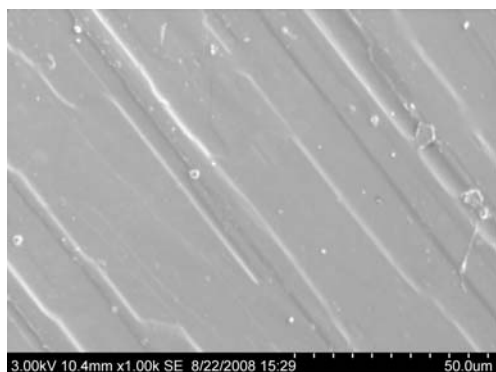


Fig. 8. SEM micrograph of DBLPZ crystal.

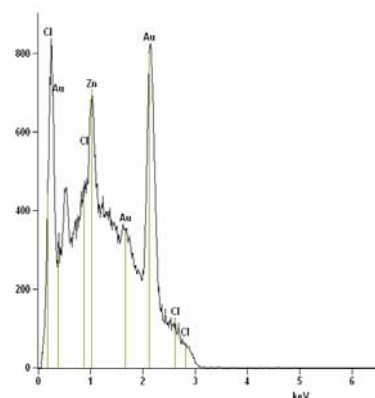


Fig. 9. EDAX spectrum of DBLPZ crystal.

3.7 SHG measurement

The powder SHG measurement was carried out for DBLPZ by Kurtz and Perry technique [8] using Nd: YAG laser with 1064 nm radiation. The crystal powder was densely packed in a microcapillary tube of diameter 1.5 mm. The laser energy incident on the capillary tube was chosen as 7.5 mJ. The SHG was confirmed by the emission of green radiation (532 nm) and the optical signal was controlled by photomultiplier tube (PMT). The optical signal incident on the PMT was converted into voltage output in the CRO. The results obtained for DBLPZ show a powder SHG efficiency of about 1.5 times that of KDP. The results were compared with other NLO materials as shown in Table 1. Fig. 10 shows powder SHG measurement of DBLPZ by Kurtz and Perry technique.

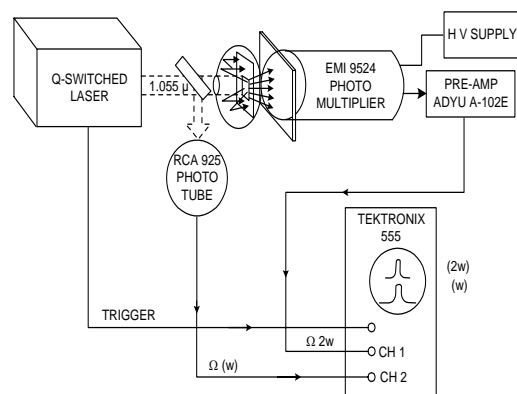


Fig. 10. Powder SHG measurement of DBLPZ by Kurtz and Perry technique.

Table 1. SHG efficiencies of DBLPZ and other semiorganic NLO crystals relative to potassium dihydrogen phosphate (KDP) equaling 1.0.

Compound	SHG efficiency	Reference
KDP	1.0	-
DBLPZ	1.5	-
Dichloridodiglycine zinc dihydrate	0.5	3
L-proline cadmium chloride monohydrate	2.0	4
L-proline lithium chloride monohydrate	0.2	5
L-alanine cadmium chloride	1.5	9
Glycine zinc sulphate	0.7	10
Glycine lithium sulphate	0.75	11
Glycine zinc chloride	0.5	12

4. Conclusion

The potential semiorganic nonlinear optical crystal of dichlorobis(L-proline)zinc(II) was grown by slow cooling technique. Single crystal X-ray diffraction study revealed that the dichlorobis(L-proline)zinc(II) crystal belongs to orthorhombic system. The morphology of the grown crystal indicates that (010) is the most prominent plane. Optical absorption studies showed that the grown crystal is optically transparent in the visible region with the lower cut-off at 235 nm and hence it is suitable for frequency conversion applications. The presence of various functional groups was confirmed by Fourier transform infrared analysis. Thermal analysis indicates that the crystal has good thermal stability. A sharp peak observed at 247.4°C in the differential scanning calorimetric curve corresponds to the melting of the material. The presence of zinc and chlorine in the crystal lattice was confirmed by energy dispersive X-ray analysis. Scanning electron microscopy reveals the step growth pattern along (010) plane. The second harmonic generation efficiency of dichlorobis(L-proline)zinc(II) is 1.5 times that of potassium dihydrogen phosphate. Thus dichlorobis(L-proline)zinc(II) is a promising material for nonlinear optical applications.

References

- [1] S. S. Gupte, R. D. Pradhan, O. A. Mareano, N. Melikechi, C. F. Desai, *J. Appl. Phys.* **91**, 3125 (2002).
- [2] M. Jiang, Q. Fang, *Adv. Mater.* **11**, 1147 (1999).
- [3] S. Mary Navis Priya, B. Varghese, J. Mary Linet, G. Bhagavannarayana, C. Justin Raj, S. Krishnan, S. Dinakaran, S. Jerome Das, *Cryst. Growth Des.* **8**, 1663 (2008).
- [4] A. Kandasamy, R. Siddeswaran, P. Murugakoothan, P. Suresh Kumar, R. Mohan, *Cryst. Growth Des.* **7**, 183 (2007).
- [5] T. Uma Devi, N. Lawrence, R. Ramesh Babu, S. Selvanayagam, E. Helen Stoeckli, K. Ramamurthi, *Cryst. Growth Des.* **9**, 1370 (2009).
- [6] S. Myung, M. Pink, M. H. Baik, D. E. Clemmer, *Acta Crystallogr. C* **61**, o506 (2005).
- [7] Y. Yukawa, N. Yasukawa, Y. Inomata, T. Takeuchi, *Bull. Chem. Soc. Jpn.* **58**, 1591 (1985).
- [8] S. K. Kurtz, T. T. Perry, *J. Appl. Phys.* **39**, 3798 (1968).
- [9] S. Dhanuskodi, K. Vasantha, P. A. Angeli Mary, *Spectrochim. Acta A* **66**, 637 (2007).
- [10] T. Balakrishnan, K. Ramamurthi, *Spectrochim. Acta A* **68**, 360 (2007).
- [11] T. Balakrishnan, K. Ramamurthi, *Cryst. Res. Technol.* **41**, 1184 (2006).
- [12] T. Balakrishnan, K. Ramamurthi, *Mater. Lett.* **62**, 65 (2008).

*Corresponding author: kalaicgc@gmail.com